Structural stability of higher-energy phases and its relation to the atomic configurations of extended defects: The example of Cu

L. G. Wang* and M. Šob
Institute of Physics of Materials, Academy of Sciences of the Czech Republic, Žižkova 22, CZ-616 62 Brno, Czech Republic
(Received 19 January 1999)

The total-energy calculations using a full-potential first-principles method have been performed for three displacive phase transformation modes in Cu. The structural and elastic properties of the ground-state (fcc) and higher-energy phases (bcc and $9R$), as well as the energy barrier for sliding of $\{111\}_{fcc}$ close-packed atomic planes and the stacking fault energy were obtained. Stability of higher-energy phases in the region of extended defects is discussed in detail. Examples presented are bcc and $9R$ Cu in grain boundaries and bcc Cu in pseudomorphic films at low temperatures. It is shown that the higher-energy phases, which are usually unstable, can be stabilized in the region of extended defects by certain imposed constraints.
[S0163-1829(99)00726-2]

I. INTRODUCTION

Extended defects play a significant role in crystalline solids as they control many physical and chemical properties of technological importance such as mechanical properties, recrystallization, electronic conductivity, diffusion, corrosion resistance, etc. By extended defects we usually mean such perturbations in the three-dimensional periodic arrangement of ideal structure which are, at least in principle, infinite in one or two dimensions, e.g., dislocations, cracks, antiphase boundaries, grain boundaries (GB's), interphase interfaces, etc. A surface is, in this sense, also an extended defect. We further regard cavities, large vacancy clusters, precipitates, etc. as extended defects, although their dimensions are finite. However, single vacancies, interstitials and their aggregates are excluded from this notion. A textbook example of the influence of extended defects on mechanical properties is dislocations. Due to their motion under stress, real strength of the crystalline solids is several order of magnitudes lower than the theoretical strength.

It was found in recent studies that atomic configurations in the GB region or other extended defects, e.g., in the epitaxial growth films on the substrate surfaces, may contain certain metastable structures which are different from the ground state. The $9R$ (α-Sm) structure was theoretically predicted and verified by high-resolution electron microscopy (HREM) at GB's in Ag (Ref. 1) and Cu.[2] Similarly, the bcc structure was found at certain GB's in Cu.[3,4] The bcc Cu phase has also been observed in the pseudomorphic Cu films grown on the $\{100\}$ surfaces of Pd, Pt, Ag, and Fe,[5–10] or as small precipitates in a bcc Fe matrix.[11] (The structure in the pseudomorphic Cu films on the Pd$\{100\}$ and Pt$\{100\}$ substrates is also considered to be the deformed fcc structures by some authors.[12,13]) And, for example, fcc Co was found in the thin cobalt films on Cu$\{100\}$ and Cu$\{111\}$ substrates.[14] Occurrence of such higher-energy or metastable phases at interfaces is even more likely in more complex non-cubic alloys such as TiAl. Indeed, structural features of this alloy have been observed very recently. Abe, Kumagai, and Nakamura[15] found a B19-type hcp-based structure in a Ti-48 at. % Al alloy quenched from the disordered phase, and Banerjee, Ahuja, and Fraser[16] observed a series of structural transitions in the form of changes in the stacking sequence of the close-packed atomic planes in the Ti and Al layers in Ti/Al multilayered thin films.

There is a great interest, on the theory front of materials science, in predicting the occurrence of stable or metastable phases as well as in gaining insights into the mechanisms which control the phase formation. Modern quantum theory is an effective tool for studying these problems. *Ab initio* calculations within the framework of density-functional theory (DFT) employing the local-density approximation (LDA) or the generalized gradient approximation (GGA) have been performed widely to predict the structural stability.[17–24] In such studies, the atomic numbers of the constituent atoms and, usually, some structural information are the only input data. Comparing with the empirical methods, an important advantage of first-principles calculations is that they can be applied reliably to the atomic configurations far from the equilibrium state.

Although Cu has been investigated intensively, there is still some controversy regarding the stability of its higher-energy phases, in particular of the bcc phase (see recent papers[9,10,13] and references therein). In the present paper we perform the full-potential first-principles total-energy calculations for three different phase transformation modes in Cu and discuss the structural stability of the higher-energy phases and its relation to the atomic configurations of extended defects. The first transformation path used in our calculations is the tetragonal deformation path, which is also known as the Bain's path.[25] In this path, the body-centered tetragonal (bct) structure is deformed along a $\langle 001\rangle$ axis and the high-symmetry bcc and fcc structures are contained as the special cases (see Fig. 1). This path has been used widely in the previous studies,[13,18,22,24,26–31] especially in the connection with the mechanism of the pseudomorphic epitaxial growth.[13,24,27,31] The second transformation path we employ is the trigonal deformation path which includes the simple cubic (sc) structure and fcc structure by distorting the bcc

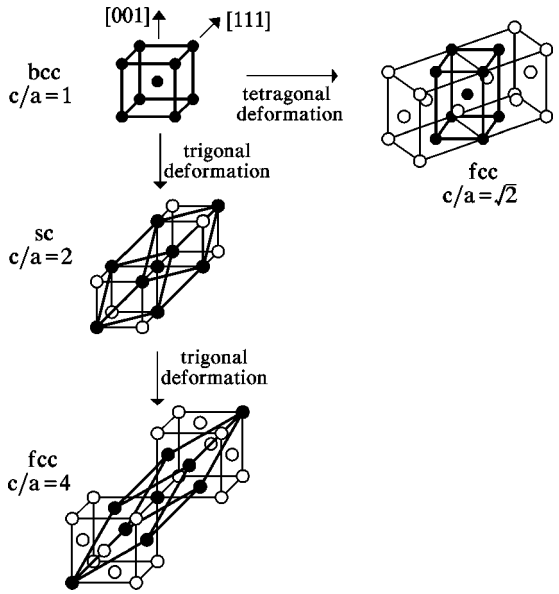

FIG. 1. High-symmetry structures obtained along the tetragonal and trigonal deformation paths. The c and a are the length scales along the deformation direction and along a perpendicular direction, respectively. For tetragonal deformation, the c axis is parallel to [001] direction and the a axis lies in the (001) plane. For trigonal deformation, the c axis points into the [111] direction and the a axis lies in the (111) plane. The body-centered cell is indicated by the filled circles and heavy solid lines.

structure along a $\langle 111 \rangle$ direction (see Fig. 1).[9,22,28,32] The third path is the fcc-to-9R transformation path which corresponds to sliding along the $\{111\}$ planes; this changes the stacking sequence of close-packed atomic planes from the fcc sequence into the sequence of 9R structure (see Sec. III D). A more complex transformation from bcc to 9R had been studied previously in investigations of the structural stability of Na at low temperatures.[33,34] These structural transformations, in which individual atoms in the unit cell or complete atomic planes in the whole crystal move to new positions in an orderly fashion, are known as displacive phase transformations or martensitic transformations.

II. COMPUTATIONAL METHOD

The full-potential linearized augmented plane wave (FLAPW) method has been proved to be one of the most accurate methods for the computation of the electronic structure of solids containing transition metals and rare-earth atoms within the density-functional theory. In this method, the basis functions inside the spheres centered at atomic sites are linear combinations of radial wave functions and their energy derivatives, and in the interstitial region they are represented by a plane-wave expansion. No shape approximations are made to the charge density and potential. Following the usual procedure, the electronic states of the system are divided into core (Cu 1s, 2s, and 2p in the present case), semicore (Cu 3s and 3p), and valence states. Core states are treated fully relativistically whereas semicore and valence states are obtained using the semirelativistic approximation. In order to improve upon the linearization (i.e., to increase the flexibility of the basis) and make possible a consistent treatment of semicore and valence states in one energy window additional basis functions (so-called ''local orbitals'') are added. We employ the WIEN95 code developed by Blaha *et al.*[35] with the exchange-correlation potential given by the PW92 scheme.[36] The muffin-tin radius is set to 2.0 a.u. Inside the atomic spheres, spherical harmonics up to $l_{max}=12$ are used to expand the wave functions, and nonspherical components of the density and potential are included up to $l_{max}=4$. We employ the energy cutoffs up to 16 Ry for the plane-wave bases and 100 Ry for star functions to describe the wave functions, the charge density, and potential in the interstitial region, respectively. The total-energy calculations for the trigonal and tetragonal deformations are performed with 8000 k points in the full Brillouin zone (BZ). 500 k points in the full BZ are utilized in the fcc-to-9R transformation, where nine atoms per unit cell had to be employed. The accuracy of the calculated structural energy difference following from the convergence tests is about 0.01 mRy/atom.

III. RESULTS AND DISCUSSION

A. Properties of the ground state

The calculated equilibrium lattice constant and the elastic properties of the ground state (fcc) Cu are shown in Table I, compared with the other calculations and the experimental values. We get the equilibrium lattice constant 3.52 Å which is in excellent agreement with the other FLAPW result[28] (see Table I). The calculated lattice constant is 2.5% smaller than the experimental value 3.61 Å,[45] which can be attributed to the deficiencies of the LDA. (In fact, if we employ the same code,[35] but with the GGA exchange-correlation potential,[38] then the equilibrium lattice constant of 3.61 Å is obtained.) The calculated bulk modulus is about 33% too large compared to the experimental value. This is also a typical deviation between the LDA calculation and the experiment.[37] The deviation between theory and experiment may also be partly due to the relativistic corrections in our calculations which are known to introduce large errors in the bulk modulus[39] (see also Table I). The shear elastic moduli C' and C_{44} agree with the experimental values within 6% and 10%, respectively.

B. Tetragonal deformation

The bct structures along the tetragonal deformation path can be parameterized in terms of the c/a ratio. If we ascribe the value $c/a=1$ to the bcc structure, then the fcc structure is obtained for $c/a=\sqrt{2}$ (see Fig. 1). We calculate the total energy with two independent variables c/a and the volume V/V_0 (V_0 is the experimental ground-state atomic volume 11.8015 Å^3). The total energy per atom as a function of c/a for various volumes is shown in Fig. 2 and the energy difference between bcc and fcc is given in the column 2 of Table II. From Fig. 2 we can see that there are three extrema in the total-energy curves with the constant atomic volumes. As it was discussed in the previous studies,[18,22] there is always an odd number of extrema; some of them are symmetry dictated. The extrema which are not dictated by the symme-

TABLE I. Calculated structural and elastic properties of fcc and bcc Cu. Lattice constants a are given in Å, elastic constants in Mbar, and structural energy differences in meV/atom. The results of the other calculations and the experimental values are presented for comparison. Both semirelativistic (SR) and nonrelativistic (NR) results from Ref. 39 are included.

	fcc				bcc			
	a(Å)	B(Mbar)	C'(Mbar)	C_{44} (Mbar)	a(Å)	B(Mbar)	C_{44} (Mbar)	E_{bcc}-E_{fcc} (meV)
This work	3.52	1.90	0.271	0.82	2.80	1.88	1.12	44.0
FLAPW (SR) [a]	3.56	1.83			2.84	1.79		48.8
FLAPW (NR) [a]	3.61	1.62			2.86	1.60		17.7
FLAPW [b]	3.52	1.90	0.250	0.80				47.6
FP-LMTO [c]	3.58	1.53	0.272	0.86	2.80		0.69	6.8
PW [d]	3.61	1.66			2.87	1.68		37.2
Expt. [e]	3.61	1.42	0.256	0.75				

[a]Ref. 39, using the Wigner exchange-correlation (xc) potential (Ref. 40).
[b]Ref. 28, using the Hedin-Lundqvist xc potential (Ref. 41).
[c]Ref. 9, using the Ceperley-Alder xc potential (Ref. 42) in the Vosko-Wilk-Nusair parametrization (Ref. 43).
[d]Ref. 13, using the Ceperley-Alder xc potential (Ref. 42) parametrized by Perdew and Zunger (Ref. 44).
[e]Refs. 45 and 46.

try usually reflect the nature of the system.[22] For the tetragonal deformation path, there are two symmetry-dictated extrema corresponding to the bcc and fcc structures. The energy of the equilibrium bcc structure is about 44.0 meV/atom higher than that of the equilibrium fcc structure, the equilibrium lattice constant being $a_{bcc}=2.80$ Å. The calculated structural energy difference is in a good agreement with the other calculations by FLAPW (Ref. 28) and by FLAPW with the semirelativistic correction (SR) (Ref. 39) (see Table I).

There is also a very shallow and flat minimum for $c/a<1$ (its position and depth varies with the volume; see Fig. 2). This minimum is imposed by the increase of total energy when c/a tends to be very small and some atoms move very close to each other. The calculated energy barrier between the equilibrium bct and fcc structures along the minimum-energy path is about 1 meV/atom (this lowest energy saddle point on the energy surface is called the transition state; we do not show our contour plot here as it is similar to Fig. 2 in the paper by Jeong[13]). The magnitude of this energy barrier is in a very good agreement with the value of 1.3 meV/atom obtained by the pseudopotential plane-wave (PW) calculations.[13] It is comparable to or smaller than thermal vibrational energies and therefore the bcc (or bct) structure is considered to be energetically unstable with respect to the tetragonal deformation. The structural instability of bcc (or bct) Cu due to the lack of the energy barrier in the tetragonal deformation was also found by other authors.[9,13,27]

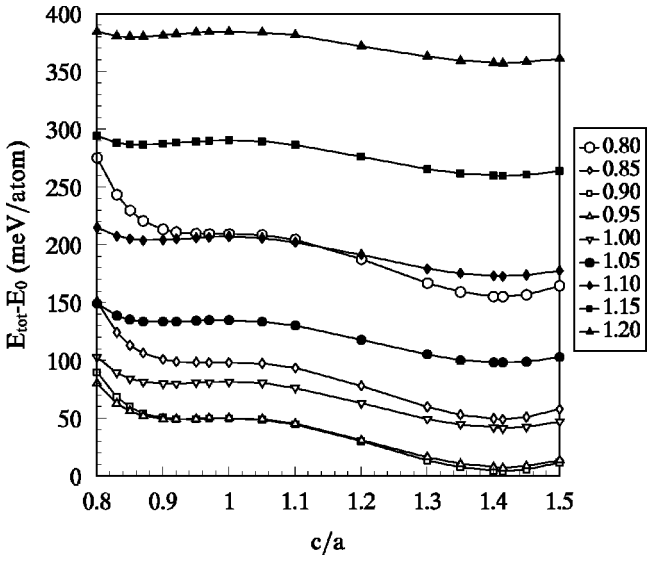

FIG. 2. Total energy per atom as a function of c/a for various values of V/V_0 along the tetragonal deformation path. V_0 is the experimental ground-state atomic volume (11.8015 Å^3), and E_0 is the total energy of equilibrium fcc Cu.

C. Trigonal deformation

In the trigonal deformation path,[22,28] we change the distance between the close-packed {111} planes, as well as the distances between the atoms in the planes, but keep their hexagonal geometry. The high symmetry bcc, sc, and fcc structures are contained as the special cases in this transformation path. Following the idea that the distortion is parametrized by c/a similarly as in the tetragonal deformation, the bcc structure is obtained for $c/a=1$, and $c/a=2$ and 4 cor-

TABLE II. The structural energy differences between the bcc and fcc structures, and between the sc and bcc structures for various atomic volumes. V_0 is the experimental ground-state atomic volume. Structural energy differences in meV/atom.

V/V_0	E_{bcc}-E_{fcc} (meV)	E_{sc}-E_{bcc} (meV)
0.80	57.4	1009.9
0.85	51.1	847.2
0.90	45.0	717.5
0.95	41.0	602.1
1.00	35.2	506.0
1.05	30.2	428.0
1.10	28.4	359.7
1.15	26.2	292.4
1.20	25.1	243.7

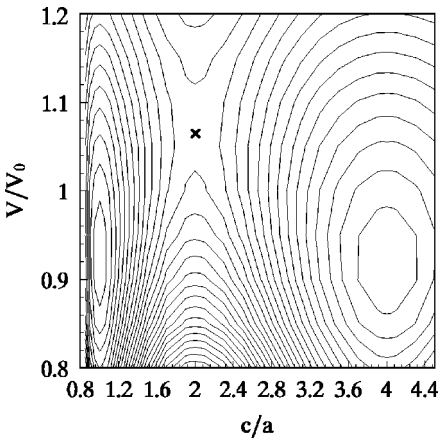

FIG. 3. Contour plot of energy surface for the trigonal deformation as a function of c/a and V/V_0. The contour spacing is 3 mRy. The cross indicates the saddle point.

respond to the sc and fcc structures on the trigonal deformation path, respectively (see Fig. 1). We calculated the total energies for this deformation from $c/a=0.8$ to $c/a=4.5$ and the volume V/V_0 varied from 0.8 to 1.2. The contour plot and the total-energy curves for various constant volumes are shown in Figs. 3 and 4. Here we can see three extrema and all of them are symmetry dictated, corresponding to the bcc, sc, and fcc structures. The bcc and fcc structures are stable with respect to the trigonal deformation. The top of a very high-energy barrier between bcc and fcc represents the sc structure.

The calculated shear modulus C_{44} for the bcc Cu is 1.12 Mbar. The energy barrier of 522.5 meV which corresponds to the energy difference between the equilibrium sc and bcc structures is much larger than the value of 115.6 meV by Kraft *et al.*[9] The saddle point or the transition state is indicated by the cross in Fig. 3. As it is shown in the previous studies,[29,48,26] the shear modulus C' of cubic transition metals correlates with the energy difference between the bcc and fcc structures. Our calculations showed that the shear modulus C_{44} is also associated with the energy difference between the sc and bcc structures for the bcc metals or with the energy difference between the sc and fcc structures for the fcc metals.[49] This can explain the difference between our value of C_{44} and that by Kraft *et al.*[9] since there is a large difference of the energy barriers between the two calculations (see also Table I). The energy differences between bcc and fcc, and between sc and bcc are strongly influenced by the atomic volume (see Table II). We can see from Table II that the structural energy difference between the bcc and fcc structures decreases with increasing atomic volume. In the region of extended defects, the volume per atom is usually larger than in the equilibrium structure, therefore we may expect that the formation of higher-energy phases, e.g., of the bcc Cu at certain GB's, costs less energy than in the perfect bulk.

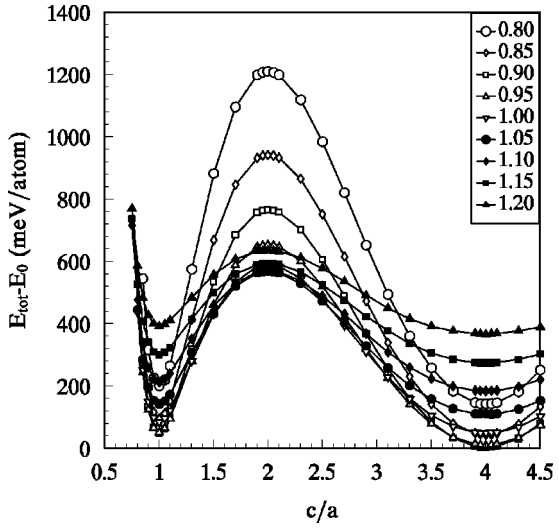

FIG. 4. Total energy per atom as a function of c/a for various values of V/V_0 along the trigonal deformation path. V_0 and E_0 are same as in Fig. 2.

D. fcc-to-9*R* transformation

The $9R$ structure consists of successive stacking of close-packed layers with the periodic sequence . . . ABCBCACAB . . . . Comparing with the fcc structure having the stacking sequence . . . ABCABCABC . . . , we can consider $9R$ as fcc with a stacking fault on every third closed-packed atomic plane. The packing fractions as well as the coordination numbers are equal in both cases. In the fcc structure, each close-packed plane is shifted by the same displacement vector with respect to the one below. The displacement of A with respect to B (and also of B with respect to C and of C with respect to A) along a certain crystallographic axis, for example a $\langle 211\rangle$ axis, is $\sqrt{6}a_{fcc}/6$. It is the same displacement, but in the opposite direction, from B to A (as well C to B and A to C). The stacking sequence of $9R$ structure may be therefore obtained by sliding the close-packed atomic planes of fcc.

The $9R$ structure has been experimentally observed in the GB's in Cu, Ag, and Au,[1,2,50] which have a low stacking fault energy. The structure in the region of the $\Sigma 3$ GB's may be $9R$ or bcc depending on the boundary inclination.[2,3] Here we perform the total-energy calculations along the fcc-to-$9R$ transformation path in Cu. In this structural transformation, the stacking sequence of close-packed atomic planes in fcc is transferred into the sequence of $9R$ by fixing the first three atomic planes, shifting the second three atomic planes by some displacement δ in the $\langle 211\rangle_{fcc}$ direction and the third three atomic planes by the same amount in the opposite direction. We parametrize the deformation by the absolute value of the shift. Here the fcc structure corresponds to the zero displacement and the $9R$ structure is obtained for $\sqrt{6}a_{fcc}/6$. Because the calculations for this deformation by a full-potential first-principles method are quite involved, we only calculated the total-energy curve for the experimental ground-state atomic volume, without performing internal relaxations (Fig. 5).

We can see that there are three extrema in the curve (Fig. 5). The fcc and $9R$ structures correspond to the minima which are dictated by the symmetry. A maximum occurs between the two minima and forms an energy barrier between the fcc and $9R$ structures. The energy of $9R$ Cu is 7.6 meV/atom higher than that of fcc Cu, which is in a very good agreement with the values of 7.2 and 6.8 meV/atom by the

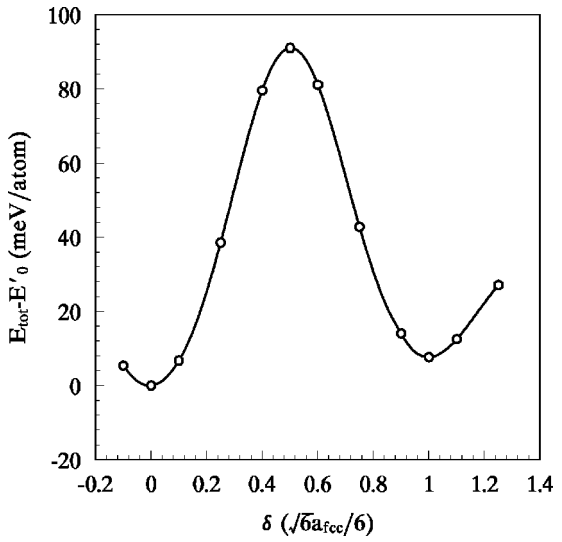

FIG. 5. Total energy per atom as a function of the absolute value of displacement along the fcc-to-9R deformation path at the experimental ground-state atomic volume. E_0' is the total energy of fcc Cu with the experimental ground-state atomic volume.

full-potential linear muffin-tin orbital (FP-LMTO) calculations.[1] The calculated energy barrier between the fcc and 9R structures is 91.0 meV/atom which is important in stabilizing the 9R structure in the $\Sigma 3$ GB's (see Sec. III E). Inclusion of internal relaxations during deformation would probably reduce the height of this barrier a little bit, but this will not change our conclusions regarding the stability of 9R structure with respect to the fcc-to-9R transformation. The fact that the energy of 9R Cu is only slightly higher than that of fcc Cu shows that the stacking fault energy in Cu is very small and therefore 9R or other stacking fault structures occur easily in the GB region. The energy difference between hcp and fcc structures following from our calculations is 10.6 meV/atom at the experimental ground-state atomic volume. This confirms the value of 10.7 meV/atom obtained by Ernst *et al.* using the FP-LMTO method.[1] The calculated intrinsic stacking fault energy is 64 mJ/m^2 which is also in excellent agreement with the value 63 mJ/m^2 by Ernst *et al.*[1] and in reasonable agreement with the experimentally estimated value 55 mJ/m^2 (Ref. 47).

E. Structural stability of higher-energy phases

Craievich and co-workers[18,19] have found that the excited phases are usually locally unstable with respect to certain deformation modes. They argued that the entropy contributions to the free energy are responsible for the stability of some of those phases at high temperatures. Our previous study[22] also showed that all higher-energy cubic structures studied are locally unstable with respect to trigonal or tetragonal deformation. But some experimental facts[7,8,10,12,14] have revealed that the higher-energy phases can be stabilized in the region of certain extended defects at room temperature and below. Thus it is an interesting issue how to understand the stability of higher-energy phases, for example, the bcc Cu in the pseudomorphic films or in the GB's, at low temperatures. In this subsection, we discuss the structural stability of higher-energy phases at low temperatures with some imposed constraints, e.g., with the epitaxial constraints in the pseudomorphic films and the internal constraints in the GB's.

For a cubic crystal, only three elastic constants, i.e., C_{11}, C_{12}, and C_{44} or the bulk modulus $B[=(C_{11}+2C_{12})/2]$, $C'[=(C_{11}-C_{12})/2]$ and C_{44} are independent. For the bcc structure, C' is the shear modulus describing the resistance of the lattice against the glide corresponding to the slip system $\{110\}\langle\bar{1}10\rangle$,[9,51] and the shear modulus C_{44} governs the glide of $\{001\}$ atomic planes in the $\langle 100\rangle$ directions.[9] We can obtain C' and C_{44} from the behavior of total energy at tetragonal and trigonal deformation, respectively. The calculated values are shown in Table I. For bcc Cu, C_{44} exhibits a finite positive value, but C' vanishes or is even negative. Thus the bcc Cu is unstable with respect to the glide of the $\{110\}$ planes. However, we can understand its stability in pseudomorphic bcc Cu films on the $\{001\}$ substrate surface.[9] Namely, the glide of $\{110\}_{bcc}$ atomic planes over each other which would take place in the bulk case is prevented here by the substrate surface which is stable and plays the role of the epitaxial constraint. And due to the finite positive C_{44}, the glide of the $\{001\}_{bcc}$ atomic planes over each other does not occur as well.

The stability of bcc Cu in the $\Sigma 3$ GB's can also be understood as following from the GB internal constraints. The atomic configurations in the region of the $\Sigma 3$ $\langle 211\rangle$ GB's may be, among others, 9R or bcc depending on the boundary inclination.[2–4] If the bcc Cu phase is formed in the GB region, the $\{111\}_{fcc}$ atomic planes in the grains become the $\{110\}_{bcc}$ atomic planes in the GB region (see, e.g., Fig. 6 of Ref. 4). Therefore the glide of the $\{110\}_{bcc}$ atomic planes in the GB region is precluded by the $\{111\}_{fcc}$ atomic planes in the grains: since the glide of the $\{111\}_{fcc}$ atomic planes in the grains cannot occur (there is an energy barrier to prevent it; see Fig. 5), the $\{110\}_{bcc}$ atomic planes in the GB region cannot glide as well. This is similar to the situation in pseudomorphic films on the $\{001\}$ substrates except the constraints in the present case are imposed on both sides of the GB region. And the relative sliding of two grains parallel to the GB plane, i.e., the glide of the $\{100\}_{bcc}$ atomic planes in the GB region (see Fig. 6 of Ref. 4) cannot take place due to the finite positive value of C_{44}. As a result, the bcc configuration in the GB's is stable.

We do not know at present what are the instability modes of the 9R structure in Cu. It cannot be excluded that this structure is even metastable, i.e., stable with respect to all small deformations from the 9R configuration. In that case, there can be a 9R-to-fcc transformation path with a much lower energy barrier than that in Fig. 5. On the basis of the above experience with the bcc structure, we may suppose that the constraints due to the presence of grains stabilize the 9R structure in the GB region in a similar manner as they stabilize the bcc structure, i.e., they prevent the movements of atoms corresponding either to an instability mode or to the 9R-to-fcc transformation with the lowest energy barrier. A more detailed analysis on the 9R structure will be the subject of future investigations.

IV. CONCLUSIONS

We have investigated the structural stability of higher-energy phases in Cu along three displacive phase transfor-

mation paths by a full-potential first-principles method. The calculated results show that bcc Cu is unstable with respect to the tetragonal deformation, but it is stable with respect to the trigonal deformation. Our study indicates that the higher-energy phases, which are usually unstable, can be stabilized by imposed constraints. Specifically, in this paper we have discussed the stabilization of bcc and $9R$ Cu in grain boundaries and of bcc Cu in pseudomorphic films. The calculated energy differences between $9R$ and fcc and between hcp and fcc are 7.6 meV/atom and 10.6 meV/atom for the experimental ground-state atomic volume, respectively. The intrinsic stacking fault energy is calculated to be 64 mJ/m^2. These results imply that the atomic configurations in the GB's in Cu may include quite complex stacking fault structures.[52]

ACKNOWLEDGMENTS

This research was supported by the Grant Agency of the Academy of Sciences of the Czech Republic (Project No. A1010817) and by the COST Action P3 ''Simulation of Physical Phenomena in Technological Applications'' (Project No. COST OC P3.10). This work is a part of activities of the Center for Computational Materials Science of the Academy of Sciences of the Czech Republic.

*On leave from the Central Iron and Steel Research Institute, Beijing 100081, China. Present address: Fritz-Haber-Institut der Max-Planck-Gesellschaft, Faradayweg 4-6, D-14195 Berlin-Dahlem, Germany. Electronic address: lgwang@fhi-berlin.mpg.de

[1] F. Ernst, M. W. Finnis, D. Hofmann, T. Muschik, U. Schönberger, and U. Wolf, Phys. Rev. Lett. **69**, 620 (1992).
[2] U. Wolf, F. Ernst, T. Muschik, M. W. Finnis, and H. F. Fischmeister, Philos. Mag. A **66**, 991 (1992).
[3] C. Schmidt, F. Ernst, M. W. Finnis, and V. Vitek, Phys. Rev. Lett. **75**, 2160 (1995).
[4] C. Schmidt, M. W. Finnis, F. Ernst, and V. Vitek, Philos. Mag. A **77**, 1161 (1998).
[5] M. H. Kang, R. C. Tatar, E. J. Mele, and P. Soven, Phys. Rev. B **35**, 5457 (1987).
[6] I. A. Morrison, M. H. Kang, and E. J. Mele, Phys. Rev. B **39**, 1575 (1989).
[7] H. Li, S. C. Wu, D. Tian, J. Quinn, Y. S. Li, F. Jona, and P. M. Marcus, Phys. Rev. B **40**, 5841 (1989).
[8] H. Li, D. Tian, J. Quinn, Y. S. Li, F. Jona, and P. M. Marcus, Phys. Rev. B **43**, 6342 (1991).
[9] T. Kraft, P. M. Marcus, M. Methfessel, and M. Scheffler, Phys. Rev. B **48**, 5886 (1993).
[10] E. H. Hahn, E. Kampshoff, N. Wälchli, and K. Kern, Phys. Rev. Lett. **74**, 1803 (1995).
[11] S. R. Goodman, S. S. Brenner, and J. R. Low, Metall. Trans **4**, 2363 (1973).
[12] Y. S. Li, J. Quinn, H. Li, D. Tian, F. Jona, and P. M. Marcus, Phys. Rev. B **44**, 8261 (1991).
[13] S. Jeong, Phys. Rev. B **53**, 13 973 (1996).
[14] Ch. Rath, J. E. Prieto, S. Müller, R. Miranda, and K. Heinz, Phys. Rev. B **55**, 10 791 (1997).
[15] E. Abe, T. Kumagai, and M. Nakamura, Intermetallics **4**, 327 (1996).
[16] R. Banerjee, R. Ahuja, and H. L. Fraser, Phys. Rev. Lett. **76**, 3778 (1996).
[17] G. W. Fernando, R. E. Watson, M. Weinert, Y. J. Wang, and J. W. Davenport, Phys. Rev. B **41**, 11 813 (1990).
[18] P. J. Craievich, M. Weinert, J. M. Sanchez, and R. E. Watson, Phys. Rev. Lett. **72**, 3076 (1994).
[19] P. J. Craievich, J. M. Sanchez, R. E. Watson, and M. Weinert, Phys. Rev. B **55**, 787 (1997).
[20] Y. Y. Ye, Y. Chen, K. M. Ho, B. N. Harmon, and P. A. Lindgard, Phys. Rev. Lett. **58**, 1769 (1987).
[21] D. Nguyen Manh, A. M. Bratkovsky, and D. G. Pettifor, Philos. Trans. R. Soc. London, Ser. A **351**, 529 (1995).
[22] M. Šob, L. G. Wang, and V. Vitek, Comput. Mater. Sci. **8**, 100 (1997).
[23] L. Cortella, B. Vinet, P. J. Desré, A. Pasturel, A. T. Paxton, and M. von Schilfgaarde, Phys. Rev. Lett. **70**, 1469 (1993).
[24] V. Ozoliņš, C. Wolverton, and A. Zunger, Phys. Rev. B **57**, 4816 (1998).
[25] E. C. Bain, Trans. AIME **70**, 25 (1924).
[26] V. L. Sliwko, P. Mohn, K. Schwarz, and P. Blaha, J. Phys.: Condens. Matter **8**, 799 (1996).
[27] P. Alippi, P. M. Marcus, and M. Scheffler, Phys. Rev. Lett. **78**, 3892 (1997).
[28] M. J. Mehl and D. A. Papaconstantopoulos, Phys. Rev. B **54**, 4519 (1996).
[29] J. M. Wills, O. Eriksson, P. Söderlind, and A. M. Boring, Phys. Rev. Lett. **68**, 2802 (1992).
[30] P. E. A. Turchi, Mater. Sci. Eng. A **127**, 145 (1990).
[31] P. M. Marcus and P. Alippi, Phys. Rev. B **57**, 1971 (1998).
[32] S. Fox and H. J. F. Jansen, Phys. Rev. B **53**, 5119 (1996).
[33] Y. Y. Ye, C. T. Chan, K. M. Ho, and B. N. Harmon, Int. J. Supercomput. Appl. **4**, 111 (1990).
[34] R. J. Gooding, Y. Y. Ye, C. T. Chan, K. M. Ho, and B. N. Harmon, Phys. Rev. B **43**, 13 626 (1991).
[35] P. Blaha, K. Schwarz, P. Dufek, and R. Augustyn, computer code WIEN95, Vienna University of Technology 1995. [Improved and updated Unix version of the original copyright WIEN code, P. Blaha, K. Schwarz, P. Sorantin, and S. B. Trickey, Comput. Phys. Commun. **59**, 399 (1990).]
[36] J. P. Perdew and Y. Wang, Phys. Rev. B **45**, 13 244 (1992).
[37] L. Fast, J. M. Wills, B. Johansson, and O. Eriksson, Phys. Rev. B **51**, 17 431 (1995).
[38] J. P. Perdew, J. A. Chevary, S. H. Vosko, K. A. Jackson, M. R. Pederson, D. J. Singh, and C. Fiolhais, Phys. Rev. B **46**, 6671 (1992).
[39] Z. W. Lu, S.-H. Wei, and A. Zunger, Phys. Rev. B **41**, 2699 (1990).
[40] E. Wigner, Phys. Rev. **46**, 1002 (1934).
[41] L. Hedin and B. I. Lundqvist, J. Phys. C **4**, 2064 (1971).
[42] D. M. Ceperley and B. J. Alder, Phys. Rev. Lett. **45**, 566 (1980).
[43] S. H. Vosko, L. Wilk, and M. Nusair, Can. J. Phys. **58**, 1200 (1980).
[44] J. P. Perdew and A. Zunger, Phys. Rev. B **23**, 5048 (1981).
[45] C. Kittel, *Introduction to Solid State Physics* (Wiley, New York, 1971).
[46] G. Simmons and H. Wang, *Single Crystal Elastic Constants and Calculated Aggregate Properties: A Handbook*, 2nd ed. (MIT Press, Cambridge, MA, 1971).
[47] P. C. J. Gallagher, Metall. Trans. **1**, 2429 (1970).

[48] P. Söderlind, O. Eriksson, J. M. Wills, and A. M. Boring, Phys. Rev. B **48**, 5844 (1993).
[49] M. Šob, L. G. Wang, and V. Vitek (unpublished).
[50] U. Wolf, P. Gumbsch, H. Ichinose, and H. F. Fischmeister, J. Phys. Colloq. **51**, C1-359 (1990).
[51] A. J. Bogers and W. G. Burgers, Acta Metall. **12**, 255 (1964).
[52] D. L. Medlin, G. H. Campbell, and C. B. Carter, Acta Mater. **46**, 5135 (1998).